SIMULATION OF AN UNITARY AIR-CONDITIONER WITH VARIABLE REFRIGERANT FLOW

Felipe Osmar Berwanger Brochier
Paulo Roberto Wander
Maria Luiza Sperb Indrusiak
UNISINOS - Mechanical Engineering Post Graduation Program, São Leopoldo, Rio Grande do Sul, Brazil
fbrochier@gmail.com
prwander@unisinos.br
mlsperb@unisinos.br

Abstract. *Since the advent of the computational era and due to its advances in hardware and software, which made possible the cost reduction and also made easier to access the high performance computers, the simulation of thermal cooling systems is becoming widely used in the industry aiming to reduce the time to market and the development costs of new air-conditioners and refrigeration systems. In the 1990's emerged the air-conditioner systems equipped with variable speed compressors controlled by frequency inverter than vary the mass flow rate of the system according to the thermal load of the ambient. Such systems offer as advantages more comfort and less energy consumption. This paper describes a computational model developed in EES software (Engineering Equation Solver), where the air-conditioner system using R-410A refrigerant was modeled with its main components: condenser, evaporator, compressor and expansion device. Simulation was performed in different conditions of outdoor temperatures, varying the compressor speed. Greater amount of heat was rejected at lower ambient temperatures, allowing reducing of the compressor speed and therefore the compression work was decreased, hence reducing the energy consumption. The model was validated with experimental tests done in a calorimeter device.*

Keywords: *air-conditioner; modeling; simulation; thermal systems; VRF*

1. INTRODUCTION

Since the advent of the computational era and due to its advances in hardware and software, which made possible the cost reduction and also made easier to access the high performance computers, the simulation of thermal cooling systems is becoming widely used in the industry aiming to reduce the time to market and the development costs of new air-conditioners and refrigeration systems. The simulation of the whole system aims not only to obtain the results of frigorific capacity of the system, or the rejected heat quantity, but also to retrieve the pressure, refrigerant temperature and mass flow, output of air temperature, air pressure drop, fan motor power, compressor motor power and other relevant data for further system analysis. Data obtained in this way help in better understanding the system behavior and the parameters that have the greatest influence in the targeted results.

Nowadays the results obtained from many vapor compression refrigerating systems allowed the advances proportionate by the computers and microprocessors used in the climate areas, food conserving, and heat pumps, making the referred systems more effective in its uses (Zigmantas, 2006).

According to Sarntichartsak et al. (2006), at the majority of the air conditioners, the cooling load is not constant. Generally, the refrigeration systems are designed to the expected peak load. The variation of load suggests that there should be some system capacity control for use during continuous system operation.

The 1990's witnessed the emergence of air conditioners provided of variable velocity compressors driven by frequency inverters, which vary the mass flow of the system accordingly to the ambient load. Sarntichartsak et al. (2006) point out that such systems offer the advantages of better indoor environment comfort and energy conservation over on/off compressor cycles.

The present study describes a computational model developed on the EES (Engineering Equation Solver) software, in which an air conditioner system using R-410A refrigerant was modeled along with its main components: condenser, evaporator, compressor and expansion device.

The system was simulated at different outdoor environment temperature conditions, also varying the compressor rotation speed. At lower temperatures the condenser has rejected greater amount of heat, making possible to reduce the compressor speed, and consequently, reducing the compressor work, hence reducing the power consumption. The model was validated with experimental tests in calorimeter.

2. VAPOR COMPRESSION REFRIGERATION CYCLE

The ideal vapor compression refrigeration cycle is constituted by four processes:
1-2 – Isentropic compression in a compressor.

2-3 – Heat rejection at constant pressure in a condenser.
3-4 – Expansion at a proper device.
4-1 – Heat absorption at constant pressure in an evaporator.

In an ideal vapor compression cycle, the refrigerant enters the compressor at state 1 as saturated vapor, being isentropically compressed until the condenser pressure, and the fluid temperature is raised above the environment value. The refrigerant enters the condenser as superheated vapor at state 2 and leaves as saturated liquid at state 3, as a result of the heat rejection to the vicinity (Çengel and Boles, 2001).

The refrigerant fluid as saturated liquid at state 3 is throttled to the evaporator pressure, due to the passage through an expansion valve or capillary tube. During this process, the fluid temperature decreases to a temperature well below the refrigerated ambient. The refrigerant enters the evaporator at state 4 as a mixture of low vapor quality, being totally vaporized due to the absorption of heat from the refrigerated space. The fluid leaves the evaporator as saturated vapor and enters again in the compressor, completing the cycle (Çengel and Boles, 2001).

The coefficient of performance of the cycle is described in Eq. (1).

$$COP = \frac{q}{w_{bal,adm}} = \frac{i_1 - i_4}{i_2 - i_1} \tag{1}$$

Where q is the cooling capacity, $w_{bal,adm}$ is the power input and i_i are the refrigerant fluid enthalpies at the boundaries of the heat exchangers.

A real frigorific cycle by vapor compression differs from the ideal in many forms, principally due to the irreversibilities that occur at the components (Çengel and Boles, 2001). One can describe amid the many irreversibilities, the pressure drop due to friction in the heat exchangers and interconnecting piping of the system, as much as the heat exchanges to the environment in compression and expansion processes. In the proposed model the expansion device is a capillary tube, hence without mass flow control.

3. CONDENSER

The condenser as described in this paper is a tube-finned heat exchanger where two distinct fluids, exchange heat separated by a surface avoiding the mixture of the fluids. The interface is done by copper micro-finned tubes assembled with interference with aluminum louvered fins, as can be seen in Fig. 1. Table 1 shows the constructive characteristics of the condenser. The analysis of the condenser presented in this paper was done considering a heat exchanger subdivided in three distinct regions: de-superheating, condensing and subcooling.
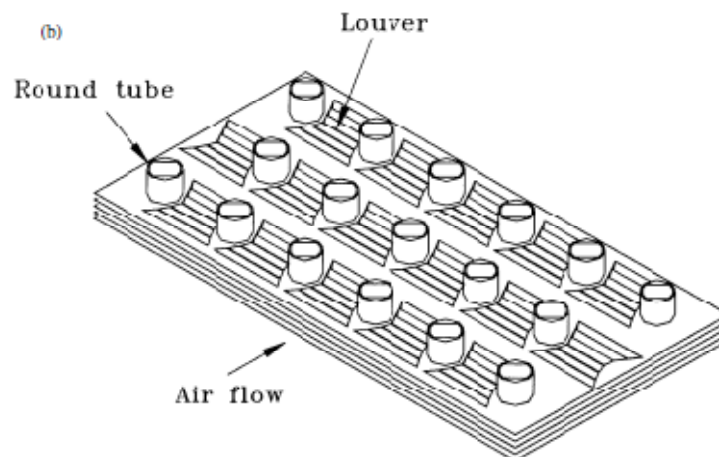

Figure 1 - Typical louver fin geometry with round tube configuration, Wang et al. (1999).

Table 1, Characteristics of the heat exchangers.

Heat Exchanger	Tube Ext. Diameter	Tube Int. Diameter	Fin Pitch	Fin thickness	Type	Length Between Sheets	Tubes per row	Number of rows
Condenser	7 mm	6.3 mm	1.27 mm	0.1 mm	Louvered	836.4 mm	22	1
Evaporator	7 mm	6.3 mm	1.59 mm	0.1 mm	Louvered	540 mm	12	2

3.1 Refrigerant fluid side

The de-superheating occurs starting from the entrance of the superheated refrigerant fluid in the condenser until the moment that it reaches the saturated vapor condition.

At the moment the vapor becomes saturated in the condenser starts the condensation itself. Condensation occurs when the saturated vapor get in contact with a surface at lower temperature. The most common type of condensation involved in heat exchangers is the surface condensation, where a cooled wall, at a temperature lower than the local saturation temperature of the vapor, is placed at contact with the vapor. In this situation, the vapor molecules that strike the cold surface may stick to it and condense into liquid. The resulting liquid (i.e., condensate) will accumulate in one of two ways. If the liquid wets the cold surface, the condensate will form a continuous film, and this mode of condensation is referred to as filmwise condensation. If the liquid does not wet the cold surface, it will form into numerous microscopic droplets. This mode of condensation is referred to as dropwise condensation and results in much larger heat transfer coefficients than during filmwise conditions (Kakaç and Liu, 2002).

The subcooling occurs at the moment the refrigerant fluid reaches the condition of saturated liquid, and the heat transfer at the refrigerant side is then monophasic.

Many different correlations for the three condenser regions where proposed by different authors. For the monophasic region was adopted the correlation proposed by Gnielinski apud Incropera (2003), Eq. (2).

$$Nu = \frac{(f/8)(\text{Re}_D - 1000)\text{Pr}}{1 + 12.7(f/8)^{1/2}\left(\text{Pr}^{2/3} - 1\right)} \tag{2}$$

Where f *is* the Fanning factor, Eq. (3). Re_D is the Reynolds number at the internal diameter and Pr is the Prandtl number

$$f = \left(0.79\ln(\text{Re}_D) - 1.64\right)^{-2} \tag{3}$$

For the condensation region, Shah (1979), proposed a correlation to obtain the mean coefficient of heat exchange inside tubes, h_m [W/m²K], Eq. (4).

$$h_m = h_L\left[0.55 + \frac{2.09}{\left(P_r/P_c\right)^{0.38}}\right] \tag{4}$$

Where P_r is the refrigerant pressure, P_c is the critical pressure of the refrigerant and h_L is the liquid phase heat transfer coefficient.

Kedzierslki and Gonçalves (1999) analyzed the condensation inside micro-finned tubes with the refrigerants R-134a, R-410A, R-125 and R-32, and obtained the correlation for the local coefficient of heat transfer, Eq. (5).

$$Nu = \frac{h_{2\varphi}D_h}{k_l} = 2.256\,\text{Re}^{\beta_1}\,\text{Ja}^{\beta_2}\,\text{Pr}^{\beta_3}\left(\frac{P_r}{P_c}\right)^{\beta_4}\left[-\log_{10}\left(\frac{P_r}{P_c}\right)\right]^{\beta_5}v^{\beta_6} \tag{5}$$

Where Ja is the Jacobi number, v is the specific volume in [m³/kg] and β_i are the exponents as follow:

Felipe O. B. Brochier. Paulo R. Wander and Maria L. S. Indrusiak
Simulation of an unitary air-conditioner with variable refrigerant flow

$$\beta_1 = 0.303$$

$$\beta_2 = 0.232x$$

$$\beta_3 = 0.393$$

$$\beta_4 = -0.578x^2$$

$$\beta_5 = -0.474x^2$$

$$\beta_6 = 2.531x$$

At which x is the vapor quality of the refrigerant.

Thome et al. (2003), proposed a model based in the flow regimes, comparing the collected data for 15 different refrigerants (R-11, R-12, R-22, R-32, R-113, R-125, R-134a, R-236ea, a near zeotropic R-32/R-125 , R-404A, R-410A, propane, n-butane, iso-butane and propilene).

Due to its simplicity, at the present study was adopted the correlation proposed by Shah (1979).

The correlation adopted for prediction of the pressure drop during the phase change is the proposed by Kedzierski and Gonçalves (1999), Eq. (6) and (7).

$$f = \left[0.002275 + 0.00933 \exp\left(\frac{e/D_i}{-0.003} \right) \right] \mathrm{Re}^{-1/[4.16 + 532 \cdot (e/D_i)]} \Phi^{0.211}$$

(6)

$$\Delta p = \left(\frac{f_r (v_0 + v_i) \Delta L}{D_h} + (v_o - v_i) \right) G^2$$

(7)

Where e is the height of micro-fin [m], Φ is the two phase number, Eq. (8), v_o and v_i are respectively the outlet and inlet specific volumes of the refrigerant, ΔL is the length of the tube [m], G is the mass velocity [kg/(m² s)] and D_h is the hydraulic diameter of the tube.

$$\Phi = \frac{\Delta x i_{fg}}{\Delta L g}$$

(8)

Where i_{fg} is the latent heat of vaporization [J/kg].

3.2 Air side

The same way that happens for the interior of the tube, i.e. refrigerant side, many different correlations were proposed by different authors for the air side.

Wang et al. (1999) developed correlations for the pressure drop and heat transfer for louvered fins without the presence of condensing humidity. Because this is the same type of fin used in the discussed model, this was the adopted correlation.

The methodology adopted to estimate the total heat rejection capacity of the condenser was also the proposed by Wang et al. (1999):

1. Obtain the heat transfer coefficient h_o [W/(m² K)], of the air side of the heat exchanger, from the correlations proposed by Wang et al. (1999).
2. Calculate the fin efficiency by using the approximation of Schimidt apud Wang et al. (1999), Eq. (9) to (12).

$$\eta = \frac{\tanh(mr\Phi)}{mr\Phi}$$

(9)

where:

$$m = \sqrt{\frac{2h_o}{k_f \delta_f}}$$ (10)

$$\Phi = \left(\frac{R_{eq}}{r} - 1\right)\left[1 + 0.35 \ln\left(R_{eq}/r\right)\right]$$ (11)

Being r the tube radius including the collar fin thickness [m], R_{eq} the equivalent radius for circular fin [m], h_o the external heat transfer coefficient [W/(m² K)] and δ_f the fin thickness [m].

For tubes in line or one row:

$$\frac{R_{eq}}{r} = 1.28 \frac{X_M}{r}\left(\frac{X_L}{X_M} - 0.2\right)^{\frac{1}{2}}$$ (12)

Where X_M and X_L are geometric parameters [m].

3. Calculate the surface efficiency from the fin efficiency, η.

$$\eta_o = 1 - \frac{A_f}{A_o}\left(1 - \eta\right)$$ (13)

Being A_f and A_o the fin surface area and the total surface area [m²], respectively.

4. Obtain the heat transfer coefficients for the inner side of the tube, i.e. refrigerant side, h_i [W/(m² K)], from Eq. (2) and (4).
5. Calculate the global heat transfer resistance from the relation of Eq. (14).

$$\frac{1}{UA} = \frac{1}{\eta_o h_o A_o} + \frac{\delta_W}{k_W A_W} + \frac{1}{h_i A_i}$$ (14)

Where k_w is the thermal conductivity of the tube wall [W/(m K)], A_W is the surface area of the tube wall [m²] and δ_W is the tube wall thickness [m].

6. Obtain the *NTU* from equation (15).

$$NTU \equiv \frac{UA}{C_{min}}$$ (15)

Where C_{min} is the minimum heat capacity rate [W/K].

7. Utilize the appropriated *ε-NTU* relation to calculate the effectiveness *ε* according to the coil arrangement and circuitry, such relation may be found in the literature, as per instance Incropera and DeWitt (2003).
8. Obtain the heat transfer rate from Eq. (16).

$$\dot{Q} = \varepsilon \dot{Q}_{max}$$ (16)

The Fanning coefficient of the heat exchanger may be calculated by Eq. (17), proposed by Kays and London apud Wand et al. (1999).

$$f = \frac{A_c \rho_1}{A_o \rho_m}\left[\frac{2\Delta P}{G_c^2 \rho_1} - \left(1 + \sigma^2\right)\left(\frac{\rho_1}{\rho_2} - 1\right)\right]$$ (17)

Where A_c is the minimum free flow area [m²], ρ_1 and ρ_2 are the inlet and outlet mass density of the fluid [kg/m³], ρ_m is the mean mass density [kg/m³], G_c is the mass velocity of the air based on the minimum flow area [kg/(m² s)] and σ is the contraction ratio of the cross-sectional area, dimensionless.

4. EVAPORATOR

The constructive characteristics of the evaporator presented in this paper are similar to the condenser, being also a tube-finned type. The general information of the evaporator is presented in Tab. 1.

According to Kakaç and Liu (2002), the region of sub-cooled boiling begins at the point in which the bubbles begin to grow at the tube wall. The bubbles form on the heated surface and release themselves, and pass through the bulk on the liquid where they may condense if the bulk temperature of the liquid is below its boiling temperature. This process is known as nucleated sub-cooled boiling. Otherwise, it is called saturated nucleate boiling or two-phase convective boiling. As the amount of superheat increases, the number of nucleation sites increases and there is a rapid increase in the rate of heat transfer.

The proposed model in this paper divides the evaporator in two distinct regions, one biphasic and other super-heated.

4.1 Refrigerant fluid side

At the outlet of the expansion device, the refrigerant is changing of phase, being a biphasic mixture of liquid and vapor. The refrigerant enters the evaporator at this condition and is heated until it reaches the saturated vapor condition with vapor quality of 1.

In a similar way it happened for the condensing process, many different correlations were proposed by different authors for the evaporation process. The correlation used in this paper is the proposed by Wojtan et al. (2005), which made a bi-phasic flow pattern map during boiling in horizontal tubes. In their model they proposed a different correlation for each flow pattern. Due to its complexity the model will not be showed in this paper.

For the super-heated region of the evaporator the correlation applied is the proposed by Gnielinski apud Incropera (2003), Eq. (2).

4.2 Air side

In the evaporator, differently than in the condenser, the air is dehumidified, because the heat exchanger surface is below the dew point temperature of the entering air, this way the heat transfer correlation for the air side utilized in the condenser could not be used in the evaporator.

The correlations adopted where the proposed by Wang et al. (2000) for heat transfer in louvered fins in wet conditions. In their work they proposed a model correlating the sensible heat coefficient and the mass transfer.

The total heat absorbed by the evaporator is calculated using the same method showed in section 3.2.

5. EXPANSION DEVICE

For the expansion device, the model of an adiabatic capillary tube proposed by Hermes et al. (2010) was considered but in order to simplify the convergence of the whole system it was not applied. Although, future works should include the model to improve the simulation results and make possible the optimization of the device.

6. COMPRESSOR

The equations to obtain the capacity, $Q_{datasheet}$, and power, $W_{datasheet}$, of the compressor under rating conditions are polynomial regressions of the curves of performance provided by the compressor manufacturer. The polynomials are presented in Eq. (18) and Eq. (19).

$$Q_{datasheet} = \begin{pmatrix} \left(1.121 T_{cd}^3 - 172.2 T_{cd}^2 + 8717 T_{cd} - 143137\right) \\ + \left(-0.5994127 T_{cd}^3 + 92.22 T_{cd}^2 - 4693 T_{cd} + 79012\right) T_{ev} \\ + \left(0.1 T_{cd}^3 - 15.46 T_{cd}^2 + 789.9 T_{cd} - 13329\right) T_{ev}^2 + \\ \left(-0.00544444 T_{cd}^3 + 0.8462963 T_{cd}^2 - 43.51 T_{cd} + 738.9\right) T_{ev}^3 \end{pmatrix} \\ \left(-0.00016165 F^2 + 0.02699884 F - 0.0379812\right)$$

(18)

$$W_{datasheet} = \begin{pmatrix} \left(0.00032099T_{cd}^3 - 0.05407407T_{cd}^2 + 3.001T_{cd} - 54.67\right)T_{ev}^3 \\ + \left(-0.00801058T_{cd}^3 + 1.3379365T_{cd}^2 - 73.68T_{cd} + 1334\right)T_{ev}^2 \\ + \left(0.06559436T_{cd}^3 - 10.85T_{cd}^2 + 592.7T_{cd} - 10651\right)T_{ev} \\ + \left(-0.19060317T_{cd}^3 + 31.31T_{cd}^2 - 1677T_{cd} + 30070\right) \\ \left(0.00007197F^2 + 0.01380169F - 0.08719482\right) \end{pmatrix}$$

(19)

Where T_{cd} [°C] and T_{ev} [°C] are respectively the temperatures of condensation and evaporation of the refrigerant, and F is the actual frequency of the compressor in [Hz].

7. CONVERGENCE METHOD

To check the convergence of the system, it was made the heat balance of each process and the temperatures of condensation and evaporation were shifted at each iteration. The simulation process is represented in the flow chart of Fig. 2.
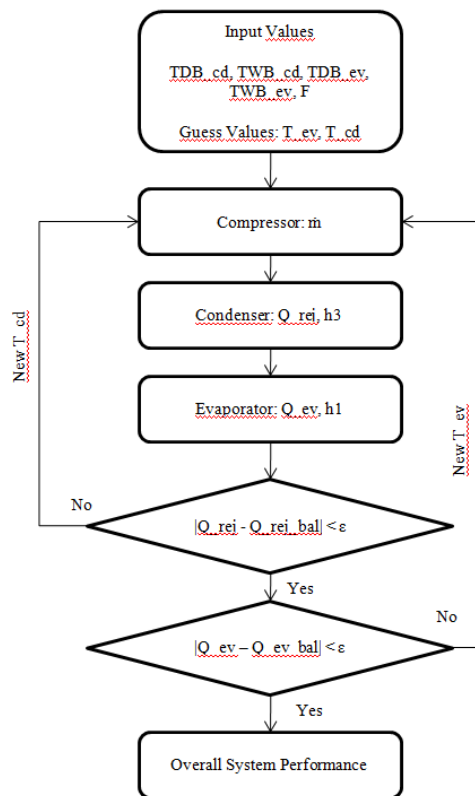

Figure 2 - Simulation Flow Chart

The heat transfer coefficients of the condenser and the evaporator were adjusted to approximate to the results obtained in the calorimeter. The overall heat transfer coefficient of the evaporator was adjusted to 67% of the estimated value and the condenser external heat transfer coefficient was adjusted to 63% of the estimated value. The compressor power input was increased in 15%.

8. RESULTS

The system was simulated in 5 different compressor speeds and for each speed, 4 different dry bulb temperatures, TDB CD, for air entering in the condenser, as seen in Tab. 2.

As one can see in Tab. 2 the air dry bulb temperature, TDB EV, and wet bulb temperature TWB EV, entering the evaporator were not changed for the different outdoor conditions.

The results of the simulations are also showed in Tab. 2. One can notice that with the diminution of the TDB CD, the cooling capacity, Q EV, increases, this happens because of the enlargement of the mean logarithm temperature between the air and the refrigerant at the condenser, which increases the heat rejection, Q REJ and decreases the evaporation temperature. As the heat rejection capacity increases, the condensation temperature of the refrigerant decreases approaching the compressor pressures of suction and discharges. The reduction of the pressure difference decreases the power input.

Table 2, Results of the simulations for different ambient conditions

TDB CD [C]	TDB EV [C]	TWB EV [C]	F [Hz]	Q REJ [W]	Q EV [W]	W [W]	COP
35	26.7	19.4	49	3026.05	2309.72	716.33	3.22
30	26.7	19.4	49	3201.97	2509.98	692	3.63
25	26.7	19.4	49	3426.15	2822.32	603.84	4.67
20	26.7	19.4	49	3645.08	3085.56	559.52	5.51
35	26.7	19.4	52	3124.42	2358.63	765.79	3.08
30	26.7	19.4	52	3293.85	2536.48	757.37	3.35
25	26.7	19.4	52	3512.75	2854.56	658.19	4.34
20	26.7	19.4	52	3719.9	3111.55	608.34	5.11
35	26.7	19.4	62	3444.86	2462.13	982.73	2.51
30	26.7	19.4	62	3680.73	2691.55	989.18	2.72
25	26.7	19.4	62	3805.74	2942.75	862.99	3.41
20	26.7	19.4	62	3964.35	3189.88	774.47	4.12
35	26.7	19.4	70	3704.21	2510.55	1193.66	2.1
30	26.7	19.4	70	3894.73	2751.53	1143.19	2.41
25	26.7	19.4	70	4026.34	2993.09	1033.25	2.9
20	26.7	19.4	70	4150.72	3223.16	927.56	3.47
35	26.7	19.4	74	3563.86	2231.3	1332.56	1.67
30	26.7	19.4	74	4013.37	2778.8	1234.57	2.25
25	26.7	19.4	74	4138.91	3006.17	1132.75	2.65
20	26.7	19.4	74	4233.12	3236.17	996.94	3.25

The cooling capacity increases, because the evaporating temperature decreases enhancing the log mean temperature of the evaporator and also increasing the mass flow.

As the frequency of the compressor increases, the mass flow of the system also increases, as well as the cooling capacity and also the power input. With the enhancement of the amount of mass circulating in the system, the condenser approach to its limit of heat rejection and the condensing temperature increases. The conclusion is that the higher the frequency the lower the COP of the system.

9. CONCLUSION

The simulation results showed good agreement to the tests made in calorimeter, demonstrating that is possible to evaluate the performance of the system in different conditions. Considering the time and money expended to perform a calorimeter test it is essential to have good software simulation during the design and development phase of a project. It is also clear, considering the necessity of adjustments, that a simulation is a support tool, and hence, its results cannot be taken as absolute values and always should be validated by testing.

The simulation tools can consistently decrease the time to market and costs of development of a project. Further studies can also take advantage of the possibilities of simulation to optimize the system with advanced heuristics methods.

10. REFERENCES

Çengel, Y. A., Boles, M. A., 2001. *Termodinâmica.* McGraw-Hill, Portugal, 3rd edition.

Hermes, C. J. L., Melo, C., Knabben, F. T., 2010. "Algebraic solution of capillary tube flows Part I: Adiabatic capillary tubes". *Applied Thermal Engineering.* v. 30.

Incropera, F. P., DeWitt, D. P., 2003. *Fundamentos de transferência de calor e de massa.* LTC, Rio de Janeiro, 5th edition.

Kakaç, S. and Liu, H., 2002. *Heat exchangers: selection, rating, and thermal design.* CRC Press, Boca Raton, 2nd edition.

Kedzierski, M. A., Gonçalves, J. M., 1999. "Horizontal convective condensation of alternative refrigerants within a micro-fin tube". *Enhanced Heat Transfer*, v. 6.

Sarntichartsak, P. et al., 2006. "Simulation and experimental evaluation of effects of oil circulation in an inverter air conditioning system using R-22 and R-407C". *Applied Thermal Engineering*.

Shah, M. M., 1979. "A general correlation for heat transfer during film condensation inside pipes. *International Journal of Heat and Mass Transfer*, V. 22.

Thome, J. R.; El Hajal, J., Cavallini, A., 2003. "Condensation in horizontal tubes, part 2: new heat transfer model based on flow regimes. *International Journal of Heat and Mass Transfer.* v. 46.

Wang, C-C et al., 1999. "Heat transfer and friction correlation for compact louvered fin-and-tube heat exchangers". *International Journal of Heat and Mass Transfer.* v. 42.

Wang, C-C, Lin, Y., Lee, C., 2000. Heat and momentum transfer for compact louvered fin-and-tube heat exchangers in wet conditions". *International Journal of Heat and Mass Transfer.* v. 43.

Wojtan, L., Ursenbacher, T., Thome, J. R., 2005. "Investigation of flow boiling in horizontal tubes: Part II - Development of a new heat transfer model for stratified-wavy, dryout and mist flow regimes". *International Journal of Heat and Mass Transfer.* v. 48.

Zigmantas, P. V. M., 2006. "Simulação de sistemas de simples estágios de refrigeração por compressão de vapor" MSc. dissertation, Universidade Federal do Pará, Belém.

11. RESPONSIBILITY NOTICE

The authors are the only responsible for the printed material included in this paper.